Dihydromyricetin Inhibits Activation of Hepatic Stellate Cells Induced by Iron Overload Through Potential Inhibition of Ferritinophagy[*]

ZENG Bin[1)**], ZHOU Shou-Hong[2,3)**], XU Zi-Wei[1,4)**], CHU Yu-Yang[5)], DUAN Wu-Xia[1,6)]

([1)]*Department of Gastroenterology, First Affiliated Hospital of University of South China, Hengyang* 421001, *China;*

([2)]*Guangxi Key Laboratory of Brain and Cognitive Neuroscience, Guilin Medical University, Guilin* 541199, *China;*

([3)]*Guangxi Key Laboratory of Diabetic Systems Medicine, Guilin Medical University, Guilin* 541199, *China;*

([4)]*Department of Gastroenterology, TheFourth People's Hospital of Changde City, Changde* 415000, *China;*

([5)]*Feinberg School of Medicine, Northwestern University, Chicago, IL* 60611, *USA;*

([6)]*Department of Gastroenterology, People's Hospital of Youxian, Zhuzhou* 412300, *China)*

Abstract **Objective** Hepatic stellate cells (HSCs) are the main producers of fibrotic extracellular matrix (ECM) and play a critical role in the initiation, progression, and regression of hepatic fibrosis (HF). Dihydromyricetin (DMY) has hepatoprotective properties, but the mechanism of this protection is unclear. Our study examined the effects of DMY on the activation of HSCs triggered by ferric ammonium citrate (FAC) in HSC-T6 cells and explored the possible mechanisms of the hepatoprotective properties of DMY. **Methods** Cell viability was evaluated using MTT assay. The levels of ECM in the culture supernatant were examined usingenzyme linked immunosorbent assay. The iron deposition levels in HSC-T6 cells were assessed using Prussian Blue staining. The total iron and free iron levels in HSC-T6 cells were measured using colorimetric assay and calcein-AM assay, respectively. The ultrastructure of HSC-T6 cells was observed using transmission electron microscopy. The expression levels of ferritin heavy chain 1 (FTH1), α-smooth muscle actin (α-SMA), nuclear receptor coactivator 4 (NCOA4), microtubule-associated protein 1 light chain 3(LC3), and p62/SQSTM1 were measured using Western blotting. **Results** Compared with the FAC group, the DMY+FAC group had a significant reduction in the main components of ECM, total iron and free ironlevels, expression levels of α-SMA, NCOA4, and LC3-II proteins, and the ratio of LC3-II/LC3-I；there was also a significant upregulation of the protein expression levels of FTH1 and p62. Furthermore, rapamycin partially blocked the effects of DMY, which inhibited the activation of HSCs induced by FAC. **Conclusion** DMY inhibits the activation of HSCs induced by iron overload, and the underlying mechanism may be involved in the inhibition of ferritinophagy.

Key words dihydromyricetin, hepatic stellate cell, iron overload, ferritinophagy, hepatic fibrosis
DOI：10.16476/j.pibb.2021.0189

Hepatic fibrosis (HF) is the common pathophysiological basis of numerous chronic liver diseases[1]. HF triggers greater synthesis than decomposition of the extracellular matrix (ECM), which results in the deposition of ECM in the liver, thus destroying the hepatic structure and leading to cirrhosis and liver failure[2-3]. Currently, the clinical treatments for HF are few in number and of limited efficacy. Therefore, elucidating the pathogenesis of HF, identifying novel effective treatments, and preventing the development of HF have become research hotspots in the field of liver diseases.

Hepatic stellate cells (HSCs) are the main producers of fibrotic ECM[4]. The activation of HSCs

is the initial step in the development of HF. HSCs mainly exist in the Disse space of the liver, accounting for 5%−15% of the total number of hepatocytes[5-6]. In the process of HF, HSCs transform into myofibroblast-like cells. The expression of myogenic marker proteins and the loss of large quantities of lipid droplets containing triacylglycerol and retinol ester are the important features of HSC activation[7-8]. α-Smooth muscle actin (α-SMA) is a sensitive and reliable marker protein for HSC activation, whereby HSC activation results in the upregulation of α-SMA expression[9]. Moreover, iron overload plays an important role in the activation of HSCs[10]; in HF, iron overload is often inevitable and leads to different degrees of HF in patients with thalassemia. Ferritin participates in the storage and release of iron and comprises 24 subunits with a combination of ferritin heavy chain 1 (FTH1) and light chains. When intracellular iron levels are low, ferritin is degraded, thus releasing iron for use by the cell[11]. Ferritinophagy is a subtype of cell autophagy, and is a selective autophagy with nuclear receptor coactivator 4 (NCOA4) as a cargo receptor, which mediates the degradation of ferritin[12-13]. During ferritinophagy, ferritin is delivered to the autophagosome by NCOA4, and this is followed by the membrane association of microtubule-associated protein 1 light chain 3 (LC3) and conversion of cytoplasmic LC3-I to phosphatidylethanolamine-bound LC3-Ⅱ. Ferritinophagy releases ferritin-bound iron[14-15]. A moderate level of ferritinophagy maintains the balance of intracellular iron, whereas excessive ferritinophagy leads to intracellular iron overload[16].

Ampelopsis grossedentata (Hand. -Mazz.) W. T. Wang is traditionally used to alleviate respiratory infections, asthma, coughs, colds, and sore throats in southern China[17]. Dihydromyricetin (DMY) is the most abundant (~30%) flavonoid extracted from *Ampelopsis grossedentata* (Hand.-Mazz.) W.T. Wang[18]. DMY possesses numerous bioactive properties, including anti-inflammatory, anti-oxidative, anti-atherosclerotic, and anti-cancer effects. It can also decrease blood glucose, enhance immunity, and protect against bone loss[19-21]. Previous studies have suggested that DMY possesses hepatoprotective effects. For example, Qiu *et al.* [22] found that DMY alleviates ethanol-induced hepatic injury. Furthermore, Zeng *et al.* [23] reported that DMY

ameliorates nonalcoholic fatty liver disease by improving mitochondrial respiratory capacity and redox homeostasis through the modulation of sirtuin 3 signaling. Guo *et al.*[24] demonstrated that DMY exerts a protective effect on the fatty liver through the NF- κB/p53/Bax signaling pathways in a rat model. However, whether DMY can inhibit HF remains unclear. We hypothesized that DMY inhibits the activation of HSCs induced by iron overload and the occurrence of HF by inhibiting the ferritinophagy pathway. To explore this possibility, we used ferric ammonium citrate (FAC) to induce iron overload and the activation of HSCs in HSC-T6 cells. Thereafter, the effects of DMY on iron overload and the activation of HSC-T6 cells were examined. Our results demonstrate that DMY inhibits the activation of HSCs induced by iron overload through potential ferritinophagy pathway.

1　Materials and methods

1.1　Cell culture and treatment

The rat hepatic stellate cell line of HSC-T6 (Xintai Jiahe Biotech Co., Ltd.) was used in this study. HSC-T6 cells were cultured in Dulbecco's modified eagle medium (Invitrogen, Inc.) containing 10% calf serum (Invitrogen, Inc.), 100 U/ml penicillin, and 0.1 g/L streptomycin (Sigma-Aldrich; Merck KGaA) and were maintained at 37°C in a humidified atmosphere of 5% CO_2. Upon reaching 70%−80% confluence, the cells were harvested and seeded into 6-well plates at a density of 1.0×10^6 cells per well. The cells were randomly divided into 6 groups: control, FAC (Shanghai Macklin Biochemical Co., Ltd.), DMY (Sigma-Aldrich; Merck KGaA), FAC+DMY, rapamycin (Sigma-Aldrich; Merck KGaA), and FAC+DMY+rapamycin. DMY was extracted *via* the solvent method[25]. The molecular formula of DMY is $C_{15}H_{10}O_8$; its molecular mass is 318.24 u, and its melting point is 357−360°C. DMY materializes as pure white acicular crystals. The experimental design for the cells in each group is shown in Table 1.

1.2　Detection of cell viability using MTT assay

The cell viability of HSCs was evaluated using MTT assay (Sigma-Aldrich; Merck KGaA) after the cell suspension was prepared. The cell density was adjusted to 5×10^5 cells/ml, and the cells were seeded in a 96-well cell culture plate. The cells were incubated with MTT (5 g/L) for 4 h, and 100 μl of

Table 1　Experimental design for the cells in each group

Group	Experimental project
Control	The cells were cultured in DMEM for 24 h
FAC	The cells were cultured in DMEM containing FAC (400 μmol/L) for 24 h[26]
DMY	The cells were cultured in DMEM containing DMY (40 mg/L) for 24 h
FAC+DMY	After the cells were incubated in DMEM containing DMY (40 mg/L) for 0.5 h, FAC (400 μmol/L) was added to the medium, and the cells were continually co-treated with DMY and FAC for 24 h
Rapamycin	The cells were cultured in DMEM containing rapamycin (100 nmol/L) for 24 h[27]
FAC+DMY+rapamycin	After the cells were incubated in DMEM containing rapamycin (100 nmol/L) for 0.5 h, DMY (40 mg/L) was added to the medium, and the cells were continually co-incubated with rapamycin and DMY for 0.5 h. Subsequently, FAC (400 μmol/L) was added to the medium, and the cells were continuallyco-incubated with rapamycin, DMY, and FAC for 24 h

DMEM: Dulbecco's modified eagle medium; DMY: dihydromyricetin; FAC: ferric ammonium citrate.

dimethyl sulfoxide was added to each well. The detection wavelength was set at 490 nm. The absorbance (*A*) was measured at a wavelength of 570 nm with an ELX-800 microplate assay reader (BioTek).

1.3　Prussian Blue iron staining

The cells were seeded in a 6-well culture plate. The cell slides were washed three times with PBS and fixed with 4% polyformaldehyde for 20 min. Thereafter, the cell slides were stained with Prussian Blue (Sigma-Aldrich; Merck KGaA) dye solution at 37° C for 30 min and then washed with deionized water. Next, the cell slides were dyed with a nuclear fixing red (Sigma-Aldrich; Merck KGaA) dye solution for 5−10 min. The cell slides were then dehydrated, sealed, dried, and placed under a microscope to assess the deposition of blue particles.

1.4　Intracellular iron colorimetric assay

The cells were collected in a test tube and 0.3% Triton X-100 was added. The cell membranes were ruptured, and the supernatant was collected by centrifugation at 4°C for 15 min at 10 000×*g*. Next, 50 μl of standard solution and 50 μl of supernatant were added to 96-well plates. Per the assay kit's instructions (Amyjet Technology Co., Ltd.), the working liquids A, B, and C were added in turn at a 1∶1∶1 ratio. All samples were mixed well and incubated for 1 h at 60°C. The *A* value was measured at a wavelength of 550 nm with an ELX-800 microplate assay reader. The relative level of total intracellular iron was calculated with reference to the *A* value of the control group set as 100%.

1.5　Intracellular free iron detection

The cells in the logarithmic growth stage were planted in 6-well cell culture plates with a cell density of 1×10⁶ cells/ml. The cells were cultured in an incubator containing 5% CO_2 at 37°C. Next, the cells were collected by adding trypsindigestive juice and centrifuged at 2 000×*g* for 5 min. The cells were incubated with 0.5 μmol/L calcein-AM (Sigma-Aldrich; Merck KGaA) at 37°C for 30 min. The mean fluorescence intensity (MFI) value was measured using an enzyme-labeled instrument (Molecular Devices) to obtain the first MFI value. The cells were then incubated withthe iron chelating agent deferiprone (100 μmol/L) for 1 h, and the second MFI value was measured using anenzyme-labeled instrument under the same conditions. The level of free iron was reflected by the difference in MFI (ΔF). The relative level of intracellular free iron was calculated with reference to the value of ΔF in the control group set as 100%.

1.6　ELISA

The supernatant of the cell culture medium was collected after centrifugation for 5 min at 1 000 ×*g*. The levels of hyaluronic acid (HA), laminin (LN), procollagen III（PCIII）, and collagen IV（IV-C）in the supernatant were measured using ELISA (Wuhan Bio-Swamp Co., Ltd.). The experiment was conducted as per the ELISA kit's instructions. The concentrations of HA, LN, PCIII, and IV-C in the supernatant were calculated according to that of the standard curve.

1.7　Transmission electron microscopy analysis

The cells collected were fixed with 3% glutaraldehyde for 2 h at 4°C followed by 1% (*v/v*) perosmic acid; the cells were then dehydrated in an ethanol series. Ultrathin sections were placed on 400-mesh grids and double-stained with uranyl acetate and lead citrate. The ultrastructure of the cells was observed using a Hitachi H-600 transmission electron microscope.

1.8 Western blotting analysis

The cells were collected and lysed on ice. Protein concentrations were measured using bicinchoninic acid assay (Pierce; Thermo Fisher Scientific, Inc.). Thereafter, the protein samples were subjected to SDS-PAGE at room temperature. Following electrophoresis, the proteins were transferred electrophoretically to PVDF membranes (Pierce; Thermo Fisher Scientific, Inc.). The PVDF membranes were blocked with 3% fat-free milk for 1 h at 37°C. Next, the blots were incubated with rabbit anti-rat FTH1 (1∶300), LC-3 (1∶200), p62 (1∶200), α-SMA (1∶400), NCOA4 (1∶300), and β-actin (1∶500) monoclonal antibodies (Santa Cruz Biotechnology, Inc.) at room temperature overnight. Subsequently, the membranes were incubated with a horseradish peroxidase-conjugated secondary antibody for 2 h at room temperature. Immunoreactivity was assessed by enhanced chemiluminescence. The band density was measured with Image J analysis software (Rawak Software, Inc. Germany), and the quantification of the level of the protein of interest compared with that of β-actin was achieved by densitometry analysis.

1.9 Statistical analysis

All results were expressed as means±SD and analyzed using SPSS 18.0 software (IBM). Significant differences between groups were determined using one-way ANOVA and LSD-t test for continuous variables and multiple groups. $P<0.05$ was considered to represent a statistically significant difference.

2 Results

2.1 Effect of DMY on the activation of HSC−T6 cells induced by FAC treatment

The protein expression levels of α-SMA were significantly upregulated in the FAC group compared with that in the control group ($P<0.05$). Conversely, the protein expression levels of α-SMA were significantly downregulated in the DMY+FAC group compared with that in the FAC group ($P<0.05$). There was no statistically significant difference in the protein expression levels of α-SMA between the DMY and control groups ($P>0.05$) (Figure 1a, b). DMY and FAC had no effect on the cell viability of
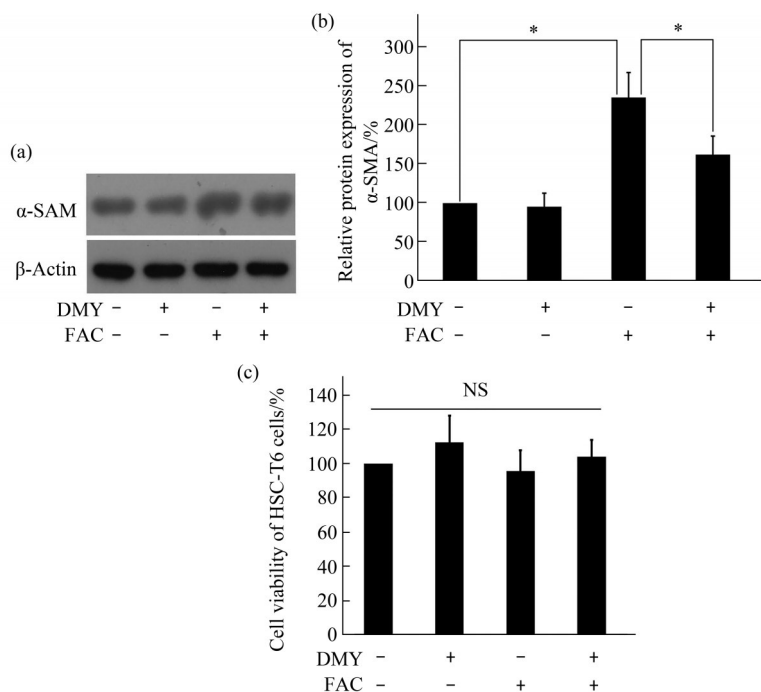

Fig. 1 Effect of DMY and FAC on the protein expression level of α−SMA and effect of DMY, FAC, and rapamycin on the cell viability in HSC−T6 cells
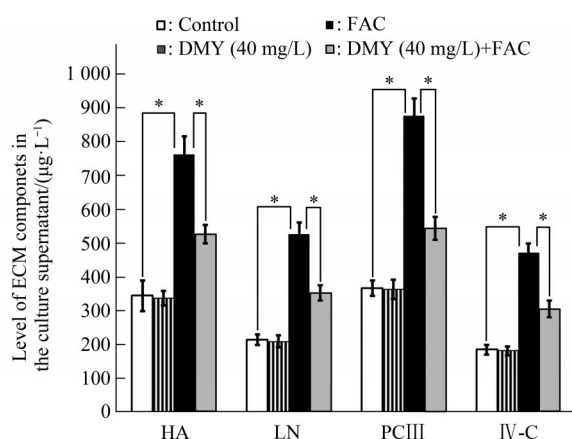
(a, b) After the HSC-T6 cells were incubated with DMEM containing DMY (40 mg/L) for 0.5 h, FAC (400 μmol/L) was added to the culture medium, and the cells were continually co-treated with DMY and FAC for 24 h. The protein expression levels of α-SMA in HSC-T6 cells was evaluated using Western blotting assay. (c) HSC-T6 cells were treated with DMY (40 mg/L), FAC (400 μmol/L), and rapamycin (100 nmol/L) for 24 h. The cell viability of HSC-T6 cells was evaluated using MTT assay. Data were presented as the mean±SD (n=3). *$P<0.05$. NS: no statistical significance. HSCs: hepatic stellate cells; DMY: dihydromyricetin; FAC: ferric ammonium citrate; α-SMA: α-smooth muscle actin.

HSC-T6 cells compared with that in the control group (all $P>0.05$)(Figure 1c).

HA, LN, PC III , and IV-C are important components of the ECM. Our results showed that the levels of HA, LN, PCIII, and IV-C in the cell culture medium were significantly increased in the FAC group compared with those in the control group (all $P<0.05$). In contrast, the levels of HA, LN, PCIII, and IV-C in the cell culture medium were significantly

decreased in the DMY+FAC group compared with those in the FAC group (all $P<0.05$). There was no statistically significant difference in the levels of HA, LN, PC III , or IV-C in the cell culture medium between the DMY and control groups (all $P>0.05$) (Figure 2). Taken together, our results suggest that DMY inhibits the activation of HSC-T6 cells induced by FAC.

Fig. 2 Effect of DMY and FAC on the levels of HA, LN, PCIII, and IV−C in the culture supernatant of HSC−T6 cells

After the HSC-T6 cells were incubated in DMEM containing DMY (40 mg/L) for 0.5 h, FAC (400 μmol/L) was added to the culture medium, and the cells were continually co-treated with DMY and FAC for 24 h. The levels of HA, LN, PCIII, and IV-C in the culture supernatant of HSC-T6 cells were examined using ELISA. Data were presented as the mean ± SD (n=3). *$P<0.05$. HSCs: hepatic stellate cells; DMEM: Dulbecco's modified eagle medium; DMY: dihydromyricetin; FAC: ferric ammonium citrate; HA: hyaluronic acid; LN: laminin; PCIII: procollagen III IV-C: collagen IV.

## 2.2 Effect of DMY on iron overload induced by FAC in HSC−T6 cells

The levels of iron deposition (Figure 3a), total iron (Figure 3b), and free iron (Figure 3c) in HSC-T6 cells were significantly increased in the FAC group compared with those in the control group (all $P<0.05$). Conversely, the levels of iron deposition, total iron, and free iron in HSC-T6 cells were significantly decreased in the DMY+FAC group compared with those in the FAC group (all $P<0.05$). There was no statistically significant difference in the levels of iron deposition, total iron, and free iron in HSC-T6 cells between the DMY and control groups (all $P>0.05$).

Our data demonstrate that DMY inhibits iron overload induced by FAC in HSC-T6 cells.

2.3 Effect of DMY on ferritinophagy induced by FAC in HSC−T6 cells

The ultrastructure of the HSC-T6 cells was observed using transmission electron microscopy. The number of autophagosomes in HSC-T6 cells was significantly increased in the FAC group compared with that in the control group ($P<0.05$). In contrast, the number of autophagosomes in HSC-T6 cells was significantly decreased in the DMY+FAC group compared with that in the FAC group ($P<0.05$)(Figure 4a). Moreover, the protein expression levels of

(a)

| Control | DMY | FAC | DMY+FAC |

(b)

(c)
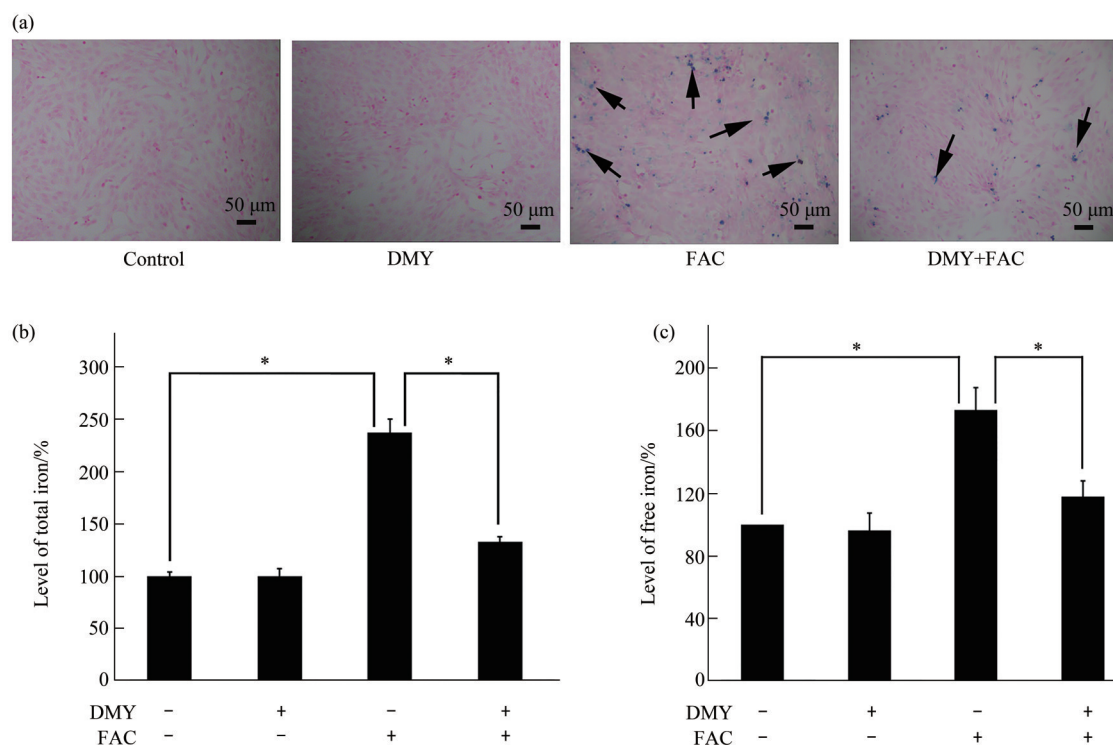
Fig. 3　Effect of DMY and FAC on the levels of iron deposition, total iron, and free iron in HSC−T6 cells

(a) After the HSC-T6 cells were incubated with DMEM containing DMY (40 mg/L) for 0.5 h, FAC (400 μmol/L) was added to the culture medium, and the cells were continually co-treated with DMY and FAC for 24 h. The iron deposition levels in HSC-T6 cells were assessed using Prussian Blue staining. The arrows represent iron deposits. (b) The levels of total iron in HSC-T6 cells were measured using colorimetric assay. (c) The levels of free iron in HSC-T6 cells were examined using calcein-AMassay. Data were presented as the mean ± SD (n=3). *P<0.05. HSCs: hepatic stellate cells; DMEM: Dulbecco's modified eagle medium; DMY: dihydromyricetin; FAC: ferric ammonium citrate.

NCOA4 (Figure 4b, c), FTH1 (Figure 4b, d), and LC3-II (Figure 4b, f), and the LC3-II/LC3-I ratio (Figure 4g) in HSC-T6 cells were significantly increased in the FAC group compared with those in the control group (all P<0.05). The protein expression levels of p62 (Figure 4b, e) in HSC-T6 cells were also significantly decreased in the FAC group compared with those in the control group (all P<0.05). Furthermore, the protein expression levels of NCOA4 and LC3-II and the LC3-II/LC3-I ratio in HSC-T6 cells were significantly decreased in the DMY+FAC group compared with those in the FAC group (all P<0.05). The protein expression levels of FTH1 and p62 in HSC-T6 cells were also significantly increased in the DMY+FAC group compared with those in the FAC group (all P<0.05). There was no statistically significant difference in the protein expression levels of NCOA4, FTH1, LC3-II, or p62, or the LC3-II/LC3-I ratio in HSC-T6 cells between the DMY (40 mg/L) and control groups (all P>0.05). Our data suggest that DMY inhibits ferritinophagy induced by FAC in HSC-T6 cells.
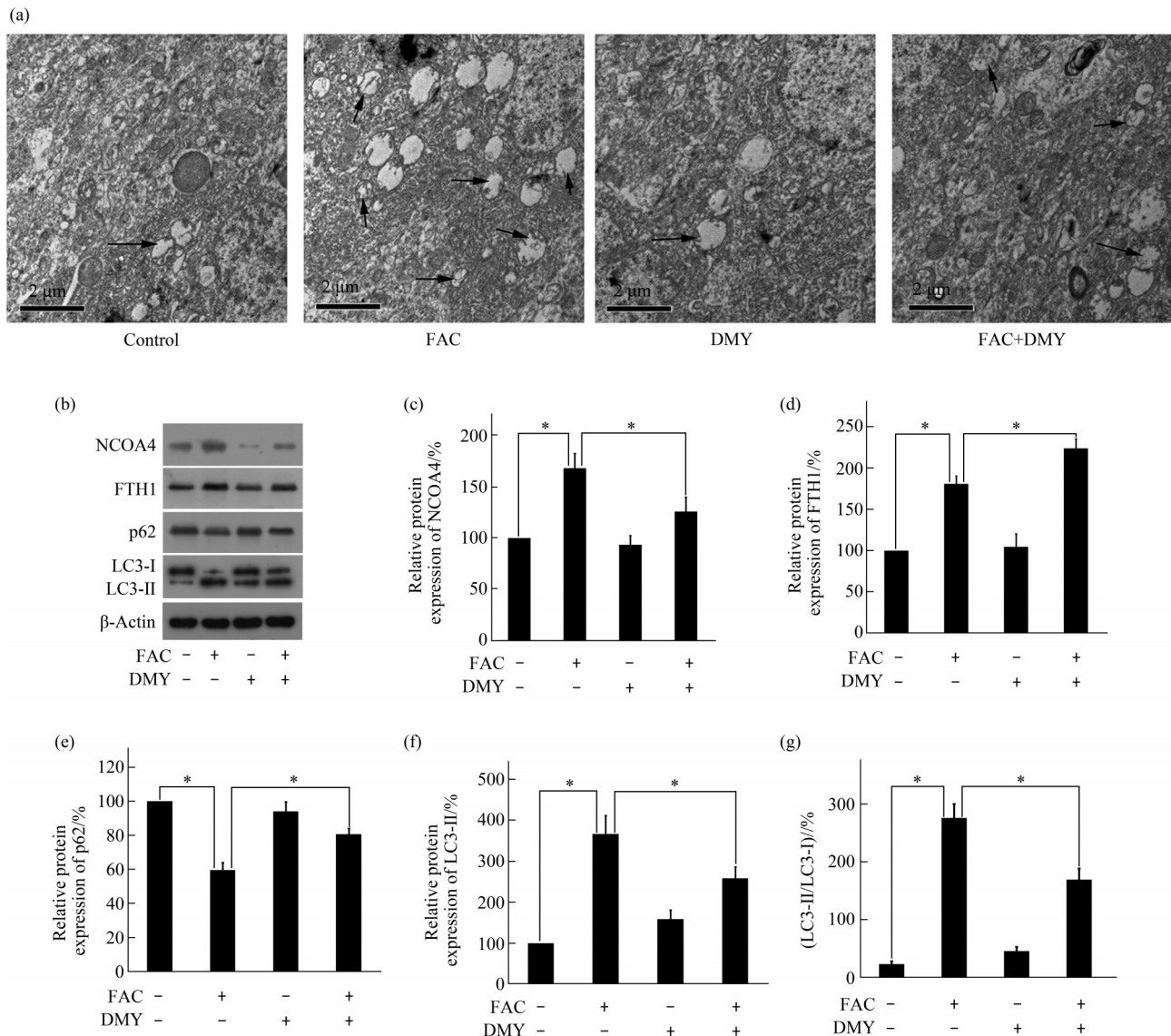
Fig. 4   Effect of DMY and FAC on autophagy and the expression levels of ferritinophagy−associated proteins in HSC−T6 cells

(a) After incubating the HSC-T6 cells in DMEM containing DMY (40 mg/L) for 0.5 h, FAC (400 μmol/L) was added to the culture medium, and the cells were continually co-treated with DMY and FAC for 24 h. The ultrastructure of HSC-T6 cells was observed using transmission electron microscopy. The arrows represent autophagosomes. (b−f) The expression levels of NCOA4, FTH1, p62/SQSTM1, and LC3-II in HSC-T6 cells were evaluated using Western blotting. (g) The ratio of LC3-II to LC3-I   was calculated. Data were presented as the mean±SD (*n*=3). *P<0.05. HSCs: hepatic stellate cells; DMEM: Dulbecco's modified eagle medium; DMY: dihydromyricetin; FAC: ferric ammonium citrate; NCOA4: nuclear receptor coactivator 4; FTH1: ferritin heavy chain 1; LC3: microtubule-associated protein 1 light chain 3.

2.4   Effect of rapamycin on the action of DMY

The protein expression levels of α-SMA (Figure 5a), the levels of HA, LN, PC Ⅲ, and IV-C in the supernatant of the cell culture of HSC-T6 cells (Table 2), and the levels of iron deposition (Figure 5b), total iron (Figure 5c), and free iron (Figure 5d) in HSC-T6 cells were significantly increased in the FAC+DMY+ rapamycin group compared with those in the FAC+

DMY group (all *P*<0.05). Rapamycin had no effect on the cell viability of HSC-T6 cells compared with that in the control group (*P*>0.05)(Figure 1c). Our results suggest that rapamycin partially blocks the effects of DMY and further confirm that DMY inhibits the activation of HSCs induced by iron overload; the underlying mechanism of this inhibitory effect of DMY may be involved in the inhibition of ferritinophagy.
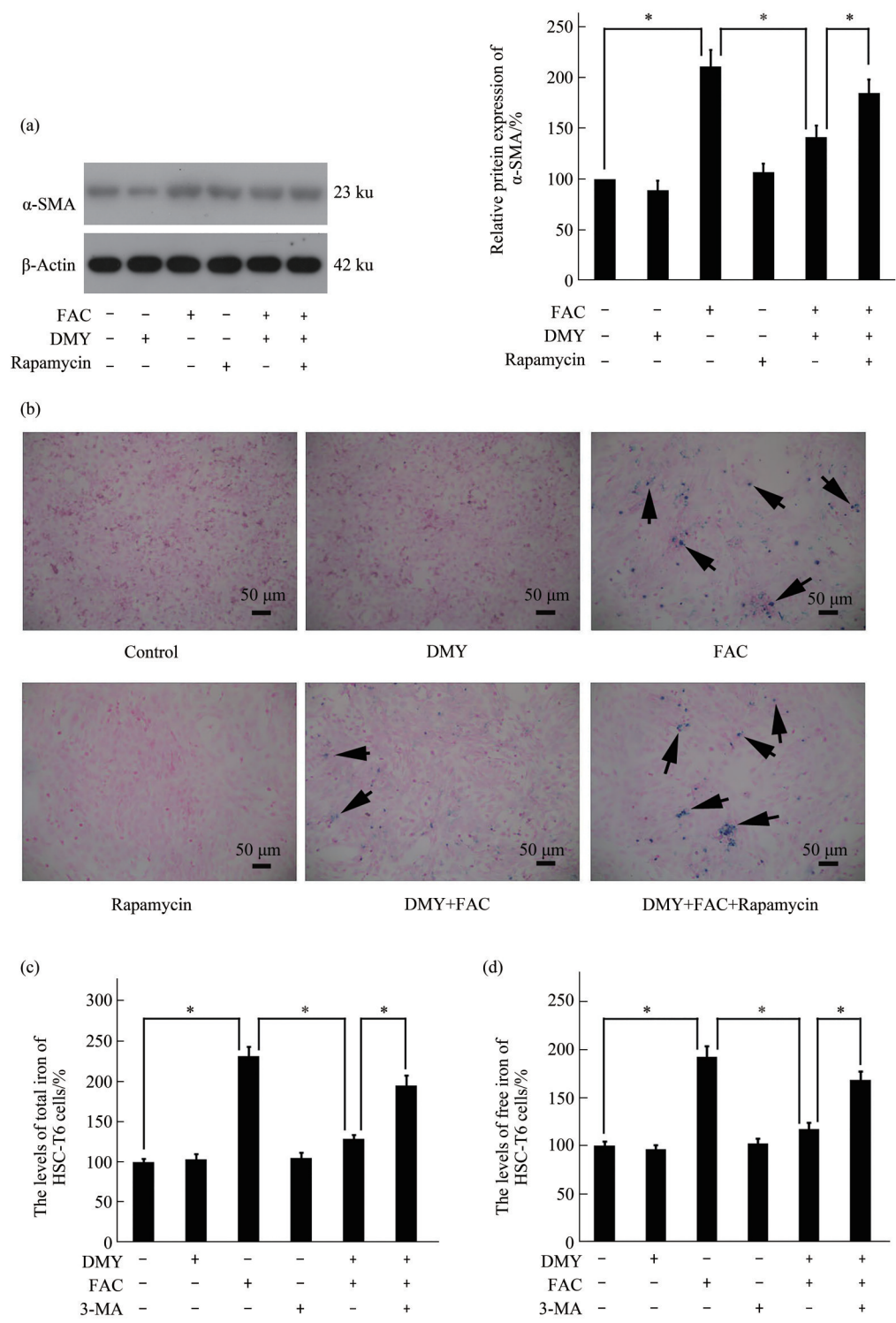
(a)

(b)

Control　　　DMY　　　FAC

Rapamycin　　　DMY+FAC　　　DMY+FAC+Rapamycin

(c)

(d)

Fig. 5　Effect of rapamycin on the action of DMY

After the cells were incubated in DMEM containing rapamycin (100 nmol/L) for 0.5 h, DMY (40 mg/L) was added to the culture medium, and the cells were continually co-incubated with rapamycin and DMY for 0.5 h. Next, FAC (400 μmol/L) was added to the culture medium, and the cells were continually co-treated with rapamycin, DMY and FAC for 24 h. (a) The protein expression of α-smooth muscle actinwas evaluated by Western blotting. (b) The iron deposition levels in HSC-T6 cells were assessed using Prussian Blue staining. The arrows represent iron deposits. (c) The levels of total iron in HSC-T6 cells were measured using colorimetric assay. (d) The levels of free iron in HSC-T6 cells were examined using calcein-AM assay. Data were presented as mean±SD (n=3). *$P<0.05$. HSCs: hepatic stellate cells; DMEM: Dulbecco's modified eagle medium; DMY: dihydromyricetin; FAC: ferric ammonium citrate; 3-MA: 3-methyladenine.

Table 2　Effect of DMY, FAC and rapamycin on the levels of HA, LN, PCⅢ and Ⅳ−C in the culture supernatant of HSC−T6 cells

Group	HA/($\mu g \cdot L^{-1}$)	LN/($\mu g \cdot L^{-1}$)	PCⅢ/($\mu g \cdot L^{-1}$)	Ⅳ-C/($\mu g \cdot L^{-1}$)
Control	367.49±31.21	224.73±12.41	384.52±26.71	195.61±12.74
DMY	346.87±24.86	217.34±14.36	361.32±31.45	187.45±15.39
FAC	746.39±52.10[*]	531.42±25.85[*]	894.10±61.02[*]	468.72±27.81[*]
Rapamycin	357.24±29.84	230.41±13.01	372.80±24.97	193.44±17.64
DMY+FAC	529.31±32.09[†]	331.63±20.14[†]	538.19±28.32[†]	310.03±24.33[†]
DMY+FAC+rapamycin	689.32±34.13[‡]	473.61±18.45[‡]	817.35±42.77[‡]	417.35±28.15[‡]

After the cells were incubated in DMEM containing rapamycin (100 nmol/L) for 0.5 h, DMY (40 mg/L) was added to the culture medium, and the cells were continually co-incubated with rapamycin and DMY for 0.5 h. Next, FAC (400 μmol/L) was added to the culture medium, and the cells were continually co-treated with rapamycin, DMY, and FAC for 24 h. The levels of HA, LN, PCIII, and IV-C in the culture supernatant of HSC-T6 cells were examined using ELISA. Data were presented as the mean±SD (*n*=3). [*]*P*<0.05 *vs.* the control group; [†]*P*<0.05 *vs.* the FAC group; [‡]*P*<0.05 *vs.* FAC+DMY group. HSCs: hepatic stellate cells; DMEM: Dulbecco's modified eagle medium; DMY: dihydromyricetin; FAC: ferric ammonium citrate; HA:hyaluronic acid; LN: laminin; PCIII: procollagen III; IV-C: collagen IV.

3　Discussion

　　Our results demonstrated that FAC-induced iron overload activated HSCs and increased the secretion of ECM through the promotion of ferritinophagy. Furthermore, DMY inhibited and decreased the FAC-induced activation of HSCs and secretion of ECM, respectively, through the inhibition of ferritinophagy. Our data suggest that DMY may serve as a new treatment for HF characterized by the activation of HSCs.

　　Previous studies have shown that HSCs play an important role in the development of HF[28-29]. The increased ECM in liver damage is mainly produced by activated HSCs. The morphological characteristics of activated HSCs include the decrease or disappearance of lipid droplets in the cells, transformation into myofibroblast-like cells, and increased expression of the marker protein α-SMA. After HSCs are activated, their proliferation rate and production of ECM and cytokines increases, whereas their apoptotic rate decreases. The ECM secreted by activated HSCs is involved in the development of HF and primarily contains HA, LN, PCⅢ, and Ⅳ-C[30]. Iron is a trace element that is essential for the growth and differentiation of various cells types in the human body. However, previous studies have shown that iron overload is closely associated with the occurrence and development of HF[31]. Excess iron induces the activation of HSCs, increases the secretion of ECM, causes collagen deposition, and leads to the development of HF[32]. Clinically, liver iron overload is related to poor prognosis for patients with HF. Iron overload not only directly induces hepatocyte death, but also leads to the activation of HSCs, which can secrete a large amount of ECM, thereby accelerating the progress of HF and increasing hepatocyte death[33].

　　Previous studies have shown that DMY has hepatoprotective properties. Xie *et al.* [32] found that DMY alleviates carbon tetrachloride-induced acute liver injury *via* a JNK-dependent mechanism in mice. Our results showed that compared with the control group, the FAC group had significantly increased protein expression levels of α-SMA in HSC-T6 cells and levels of HA, LN, PCⅢ, and IV-C in the supernatant of HSC-T6 cells. These results indicate that iron overload caused HSC activation and increased the secretion of ECM in HSCs, suggesting that our model of iron overload-induced HSC activation was successful. Moreover, DMY (20, 40, 80, 160, and 320 mg/L) significantly downregulated the protein expression levels of α-SMA and the levels of HA, LN, PCⅢ, and IV-C in HSC-T6 cells in the FAC+DMY group compared with those in the FAC group. These results indicate that DMY inhibited the FAC-induced activation of HSCs. However, the detailed mechanism for this inhibition remains unclear.

　　When hemoglobin is degraded in the cells, iron is released. Most iron is bound to ferritin and is released from the cells *via* membrane iron transporters. Iron binds to transferrin, which in turn binds to transferrin receptors on the surface of HSC membranes, and subsequently enters HSCs through phagocytosis. Iron is then released from endocytosis bodies, binding to ferritin and stored in HSCs. Ferritinophagy mediates the degradation of ferritin in

the autophagolysosome, thereby releasing ferritin-bound iron as free iron[34]. A moderate level of ferritinophagy maintains iron homeostasis, whereas excessive ferritinophagy leads to an intracellular iron overload[35]. Zhang et al.[36-37] found that activation of ferritinophagy is required for the RNA-binding protein ELAVL1/HuR to regulate ferroptosis in hepatic stellate cells and ELAVL1-autophagy-dependent ferroptosis is a potential target for the treatment of liver fibrosis and RNA-binding protein ZFP36/TTP protects against ferroptosis by regulating autophagy signaling pathway in hepatic stellate cells. Our results showed that compared with the control group, the FAC group had significantly increased number of autophagosomes in HSC-T6 cells, the expression levels of NCOA4 and LC3-II , and the LC3-II/LC3-I ratio, whereas the protein expression levels of p62 was significantly decreased. These results suggest that FAC promotes ferritinophagy in HSC-T6 cells.

FTH1 is the substrate inferritinophagy. The protein expression levels of FTH1 should be downregulated when ferritinophagy occurs[38]. However, our results showed that the expression levels of FTH1 were upregulated after FAC treatment. Intracellular protein levels depend on both the synthesis and degradation rates of the protein. FAC treatment increased the level of ferritinophagy in our results, which should have led to the increased degradation of ferritin and a decrease in FTH1 levels. A possible explanation for our results is that the increased synthesis of ferritin was induced by an unknown mechanism. FTH1 combines large quantities of iron and stores it. Although FAC induced an increase inferritinophagy, this increase was still insufficient to offset the increase in FTH1 synthesis induced by excessive iron. Therefore, the expression levels of FTH1significantly increased after FAC treatment. Further research is needed to confirm this possibility. Our results further showed that DMY treatment in HSC-T6 cells treated with FAC significantly reduced the number of autophagosomes, the expression levels of NCOA4 and LC3-II, and the ratio of LC3-II/LC3-I, but significantly increased the expression levels of FTH1 and p62. These results indicate that DMY inhibited the increase in ferritinophagy induced by FAC in HSC-T6 cells. Owing to a lack of specific inducers for ferritinophagy, our study further evaluated the effect

of rapamycin, a general inducer of cell autophagy, on the effects of DMY. The results showed that the expression levels of α-SMA protein, the levels of HA, LN, PC III , and IV-C in the cell culture supernatant, and the levels of intracellular iron deposition, total iron, and free iron significantly increased in the FAC+DMY+rapamycin group compared with those in the FAC+DMY group. These results indicate that rapamycin partially blocked the effects of DMY and suggest that DMY inhibited iron overload-induced activation of HSCs, the underlying mechanism may be involved in the inhibition of ferritinophagy.

4 Conclusion

Our results demonstrate that DMY inhibited the activation of HSCs induced by iron overload, and the underlying mechanism may be involved in the inhibition of ferritinophagy. Our results provide new insights into the prevention and treatment of HF and experimental evidence for the clinical treatment of HF with DMY.

References

[1] Li B, Feng W T, Li J Y, et al. Treatment of liver fibrosis using traditional Chinese medicine through anti-inflammatory mechanism. Prog Biochem Biophys, 2020,**47**(8):790-808

[2] Kisseleva T, Brenner D. Molecular and cellular mechanisms of liver fibrosis and its regression. Nat Rev Gastroenterol Hepatol, 2021,**18**(3): 151-166

[3] Huang C, Gan D, Luo F, et al. Interaction mechanisms between the NOX4/ROS and RhoA/ROCK1 signaling pathways as new anti-fibrosis targets of ursolic acid in hepatic stellate cells. Front Pharmacol, 2019,**10**: 431

[4] Trivedi P, Wang S, Friedman S L. The power of plasticity-metabolic pegulation of hepatic stellate cells. Cell Metab, 2021, **33**(2): 242-257

[5] Bekki Y, Yoshizumi T, Shimoda S, et al. Hepatic stellate cells secreting WFA+-M2BP: its role in biological interactions with Kupffer cells. J Gastroenterol Hepatol, 2017,**32**(7): 1387-1393

[6] Xu T, Pan L, Li L, et al. MicroRNA-708 modulates hepatic stellate cells activation and enhances extracellular matrix accumulation via direct targeting TMEM88. J Cell Mol Med, 2020, **24**(13): 7127-7140

[7] 石磊, 秦恩强, 贾雅丽, 等 . 肝星状细胞中表皮形态发生素表达调控机制及其作用研究 . 生物化学与生物物理进展, 2016, **43**(5): 506-513
Shi L, Qin E Q, Jia Y L, et al. Prog Biochem Biophys, 2016, **43**(5): 506-513

[8] Li Q, Ding Y, Guo X, *et al*. Chemically modified liposomes carrying TRAIL target activated hepatic stellate cells and ameliorate hepatic fibrosis *in vitro* and *in vivo*. J Cell Mol Med, 2019, **23**(3): 1951-1962

[9] Gaul S, Leszczynska A, Alegre F, *et al*. Hepatocyte pyroptosis and release of inflammasome particles induce stellate cell activation and liver fibrosis. J Hepatol, 2021, **74**(1): 156-167

[10] Sui M, Jiang X, Chen J, *et al*. Magnesium isoglycyrrhizinate ameliorates liver fibrosis and hepatic stellate cell activation by regulating ferroptosis signaling pathway. Biomed Pharmacother, 2018, **106**: 125-133

[11] Strbak O, Balejcikova L, Kmetova M, *et al*. Quantification of iron release from native ferritin and magnetoferritin induced by vitamins B$_2$ and C. Int J Mol Sci, 2020, **21**(17): 6332

[12] Li N, Wang W, Zhou H, *et al*. Ferritinophagy-mediated ferroptosis is involved in sepsis-induced cardiac injury. Free Radic Biol Med, 2020, **160**: 303-318

[13] Latunde-Dada G O. Ferroptosis: role of lipid peroxidation, iron and ferritinophagy. Biochim Biophys Acta Gen Subj, 2017, **1861**(8): 1893-1900

[14] Masaldan S, Clatworthy S A S, Gamell C, *et al*. Iron accumulation in senescent cells is coupled with impaired ferritinophagy and inhibition of ferroptosis. Redox Biol, 2018, **14**: 100-115

[15] Tang M, Huang Z, Luo X, *et al*. Ferritinophagy activation and sideroflexin1-dependent mitochondria iron overload is involved in apelin-13-induced cardiomyocytes hypertrophy. Free Radic Biol Med, 2019, **134**: 445-457

[16] Ajoolabady A, Aslkhodapasandhokmabad H, Libby P, *et al*. Ferritinophagy and ferroptosis in the management of metabolic diseases. Trends Endocrinol Metab, 2021, **32**(7): 444-462

[17] Carneiro R C V, Wang H, Duncan S E, *et al*. Flavor compounds in Vine Tea (*Ampelopsis grossedentata*) infusions. Food Sci Nutr, 2020, **8**(8): 4505-4511

[18] Zhou H Y, Gao S Q, Gong Y S, *et al*. Anti-HSV-1 effect of dihydromyricetin from *Ampelopsis grossedentata via* the TLR9-dependent anti-inflammatory pathway. J Glob Antimicrob Resist, 2020, **23**: 370-376

[19] 吕慧婕, 朱责梅, 陈维昭, 等. 二氢杨梅素通过下调JNK信号拮抗高糖诱导的PC12细胞凋亡. 生物化学与生物物理进展, 2018, **45**(6): 663-671
Lü H J, Zhu Z M, Chen W Z, *et al*. Prog Biochem Biophys, 2018, **45**(6): 663-671

[20] Zhou F Z, Zhang X Y, Zhan Y J, *et al*. Dihydromyricetin inhibits cell invasion and down-regulates MMP-2/-9 protein expression levels in human breast cancer cells. Prog Biochem Biophys, 2012, **39**(4): 352-358

[21] Li T, Yan F, Meng X, *et al*. Improvement of glucocorticoid-impaired thymus function by dihydromyricetin *via* up-regulation of PPARγ-associated fatty acid metabolism. Pharmacol Res, 2018, **137**: 76-88

[22] Qiu P, Dong Y, Li B, *et al*. Dihydromyricetin modulates p62 and autophagy crosstalk with the Keap-1/Nrf2 pathway to alleviate ethanol-induced hepatic injury. Toxicol Lett, 2017, **274**: 31-41

[23] Zeng X, Yang J, Hu O, *et al*. Dihydromyricetin ameliorates nonalcoholic fatty liver disease by improving mitochondrial respiratory capacity and redox homeostasis through modulation of SIRT3 signaling. Antioxid Redox Signal, 2019, **30**(2): 163-183

[24] Guo L, Zhang H, Yan X. Protective effect of dihydromyricetin revents fatty liver through nuclear factorκB/p53/B cell lymphoma 2associated X protein signaling pathways in a rat model. Mol Med Rep, 2019, **19**(3): 1638-1644

[25] Mejias M, Gallego J, Naranjo-Suarez S, *et al*. CPEB4 increases expression of PFKFB3 to induce glycolysis and activate mouse and human hepatic stellate cells, promoting liver fibrosis. Gastroenterology, 2020, **159**(1): 273-288

[26] Liu F, Zhang W L, Meng H Z, *et al*. Regulation of DMT1 on autophagy and apoptosis in osteoblast. Int J Med Sci, 2017, **14**(3): 275-283

[27] Wang Y, Yi X D, Li C D. Suppression of mTOR signaling pathway promotes bone marrow mesenchymal stem cells differentiation into osteoblast in degenerative scoliosis: *in vivo* and *in vitro*. Mol Biol Rep, 2017, **44**(1): 129-137

[28] Gao J, Wei B, de Assuncao T M, *et al*. Hepatic stellate cell autophagy inhibits extracellular vesicle release to attenuate liver fibrosis. J Hepatol, 2020, **73**(5): 1144-1154

[29] Andueza A, Garde N, García-Garzón A, *et al*. NADPH oxidase 5 promotes proliferation and fibrosis in human hepatic stellate cells. Free Radic Biol Med, 2018, **126**: 15-26

[30] Yu Y, Jiang L, Wang H, *et al*. Hepatic transferrin plays a role in systemic iron homeostasis and liver ferroptosis. Blood, 2020, **136**(6): 726-739

[31] Zhang Z L, Wang X, Wang Z L, *et al*. Dihydroartemisinin alleviates hepatic fibrosis through inducing ferroptosis in hepatic stellate cells. Biofactors 2021, **47**(5): 801-818

[32] Xie J, Liu J, Chen T M, *et al*. Dihydromyricetin alleviates carbon tetrachloride-induced acute liver injury *via* JNK-dependent mechanism in mice. World J Gastroenterol, 2015, **21**(18): 5473-5481

[33] Lainé F, Ruivard M, Loustaud-Ratti V, *et al*. Metabolic and hepatic effects of bloodletting in dysmetabolic iron overload syndrome: a randomized controlled study in 274 patients. Hepatology, 2017, **65**(2): 465-474

[34] Liu Z, Lv X, Song E, *et al*. Fostered Nrf2 expression antagonizes iron overload and glutathione depletion to promote resistance of neuron-like cells to ferroptosis. Toxicol Appl Pharmaco, 2020, **407**: 115241

[35] Tian Y, Lu J, Hao X, *et al*. FTH1 inhibits ferroptosis through ferritinophagy in the 6-OHDA model of parkinson's disease. Neurotherapeutics, 2020, **17**(4): 1796-1812

[36] Zhang Z L, Yao Z, Wang L, *et al*. Activation of ferritinophagy is required for the RNA-binding protein ELAVL1/HuR to regulate ferroptosis in hepatic stellate cells. Autophagy, 2018, **14**(12): 2083-2103

[37] Zhang Z L, Guo M, Li Y J, *et al*. RNA-binding protein ZFP36/TTP protects against ferroptosis by regulating autophagy signaling pathway in hepatic stellate cells. Autophagy, 2020, **16**(8): 1482-1505

[38] Li H, Li Y, Zhang Y, *et al*. Comparison of refluxing, ultrasonic- and microwave-assisted extraction of dihydromyricetin from ampelopsis grossedentata. J AOAC Int, 2008, **91**(6): 1278-1283

二氢杨梅素通过抑制铁自噬而抑制铁超载诱导的
肝星状细胞活化*

曾 斌 [1)**] 周寿红 [2,3)**] 许紫薇 [1,4)**] 储宇阳 [5)] 段无暇 [1,6)]

([1)] 南华大学附属第一医院消化内科，衡阳 421001；
[2)] 桂林医学院广西脑与认知神经科学重点实验室，桂林 541199；
[3)] 桂林医学院广西糖尿病系统医学重点实验室，桂林 541199；
[4)] 常德市第四人民医院消化内科，常德 415000；
[5)] *Feinberg School of Medicine, Northwestern University, Chicago, IL 60611, USA*；
[6)] 湖南省株洲市攸县人民医院消化科，株洲 412300）

摘要 目的 肝星状细胞（HSCs）是肝纤维化（HF）过程中细胞外基质（ECM）的主要来源，在HF的发生发展中起着重要作用。二氢杨梅素（DMY）具有保肝作用，但机制不清。本研究观察了DMY对枸橼酸铁铵（FAC）诱导HSC-T6细胞活化的影响，并探讨了可能的机制。**方法** 采用MTT法检测细胞活力，ELISA法检测培养上清中ECM主要成分的含量，普鲁士蓝染色观察HSC-T6细胞铁沉积，比色法测定HSC-T6细胞总铁含量，钙黄绿素法检测细胞内游离铁水平，透射电镜观察HSC-T6细胞超微结构。蛋白质免疫印迹法检测铁蛋白重链1（FTH1）、α平滑肌肌动蛋白（α-SMA）、核受体辅活化子4（NCOA4）、微管相关蛋白1轻链3（LC3）和p62/SQSTM1的表达。**结果** 与FAC组比较，DMY+FAC组细胞培养液中ECM主要成分、细胞内总铁和游离铁水平、细胞中α-SMA、NCOA4和LC3-Ⅱ表达以及LC3-Ⅱ/LC3-Ⅰ比值均显著降低，而FTH1和p62蛋白表达显著上调。雷帕霉素部分阻断DMY抑制FAC诱导的HSCs活化的作用。**结论** DMY可抑制铁超载诱导的HSCs活化，其机制可能与抑制铁自噬有关。

关键词 二氢杨梅素，肝星状细胞，铁过载，铁自噬，肝纤维化
中图分类号 R575，R965　　　　　　　　　**DOI**：10.16476/j.pibb.2021.0189